

Simulated nanojet ejection process by spreading droplets on a solid surface

This article has been downloaded from IOPscience. Please scroll down to see the full text article.

2003 J. Phys.: Condens. Matter 15 8263

(<http://iopscience.iop.org/0953-8984/15/49/005>)

View [the table of contents for this issue](#), or go to the [journal homepage](#) for more

Download details:

IP Address: 171.66.16.125

The article was downloaded on 19/05/2010 at 17:50

Please note that [terms and conditions apply](#).

Simulated nanojet ejection process by spreading droplets on a solid surface

Te-Hua Fang¹, Win-Jin Chang^{2,3} and Shi-Cheng Liao¹

¹ Department of Mechanical Engineering, Southern Taiwan University of Technology, Tainan 710, Taiwan

² Department of Mechanical Engineering, Kun-Shan University of Technology, Tainan 710, Taiwan

E-mail: changwj@mail.ksut.edu.tw

Received 11 August 2003, in final form 5 November 2003

Published 25 November 2003

Online at stacks.iop.org/JPhysCM/15/8263

Abstract

This paper studies the nanojet ejection process by spreading droplets on a solid surface using molecular dynamics simulation based on the Lennard-Jones potential. During the simulation, it was found that the spreading width increased as the aperture dimensions and time increased. An energy wave phenomenon was also found in the simulation. After the ejection process reaches a relatively steady state, the droplets' contact angle ranged from about 30° to 60°. When the atoms were deposited on a moving plate the layer phenomenon became apparent.

(Some figures in this article are in colour only in the electronic version)

1. Introduction

Jets are attracting considerable attention due to their unique characteristics. Thus, jets of microscopic dimensions have been of great scientific interest for use in many industrial applications [1–3]. However, in the nanoworld, to actually build a nanojet is still a difficult task and using molecular dynamics is an ideal tool to simulate this. Molecular dynamics simulations can contribute to a recognition of the underlying atomistic mechanisms and offer novel insights into nanometre-scale behaviour, due to their high temporal and spatial resolution [4–8]. In addition, molecular dynamics can clearly identify the atomic configuration of each nanojet trajectory.

The research concerning microscopic jets has wide application in industrial practices [9–11]; however, only a limited portion of the literature is concerned with nanojets. Moseler and Landman performed a molecular dynamics computation for a nanojet squirting propane from nozzles 2–6 nm in diameter and found that no steady jet formation was possible [12]. Recently, Eggers studied the breakup of a liquid nanojet [13]. Based on an equation derived by

³ Author to whom any correspondence should be addressed.

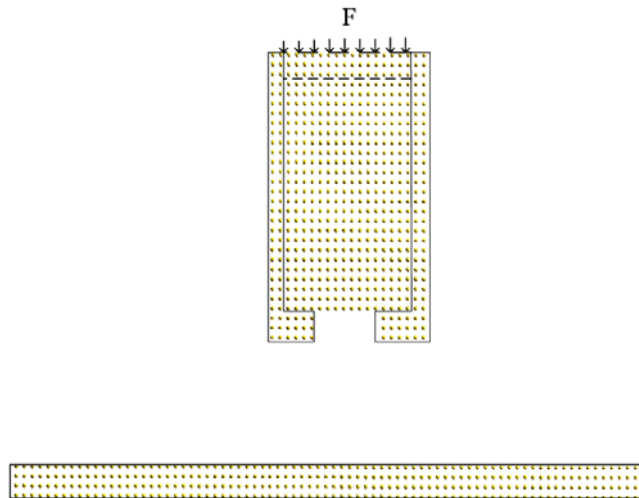


Figure 1. The nanojet system molecular dynamics model.

Moseler and Landman, Eggers showed that noise can speed up the breakup phenomenon [13]. The nozzle size also has an important effect on the control of the nanojet ejection flow rate and particle distribution. de Gennes *et al* [14, 15] follows Tanner's spreading law [16] and describes a balance between the viscous dissipation and the surface tension force. The other researchers [17, 18] studied the wetting dynamics by molecular dynamics simulation. In this study the spreading dynamics as well as the effect of the moving plate were studied.

This paper studies the spreading dynamics on a solid surface as well as the effects of the moving plate during the nanojet ejection process using different nozzle aperture dimensions. This will be useful in assisting future design and possible manufacturing of a nanosprayer or a nanoprinter and the behaviour documented can be used to improve the molecular beam jet's functionality.

2. Methodology

The spreading of argon clusters on a plate was investigated using molecular dynamics simulations. The initial atomic configuration used in the simulation system is shown in figure 1. The Ar atoms inside the housing are liquid, while the housing and the plate are made of rigid Ar atoms. F stands for the applied force. In the simulation the interaction of the Ar atoms and the housing material was taken into account.

For this simulation, the system was set as a canonical ensemble model [19]. The nanojet atomic array model is simulated under the condition of constant temperature and volume (i.e. NVT model). 624 atoms were constructed as a push panel with a velocity of 50 m s^{-1} from the back of the system and the plate was constructed with 12 800 atoms. The distance between the plate and the front of the nanojet housing was 6.2 nm.

The total atoms in table 1 represent the push panel atoms, the housing atoms, the plate atoms and the squirtable interior atoms. There are four aperture types in the simulation: they are types A, B, C and D. A, B, C and D represent the four different aperture dimensions as listed in table 1. For the simulation the still widely used Lennard-Jones potential model was used, which was adopted for the calculation process [20]. It is

$$\phi(r_{ij}) = 4\epsilon \left[\left(\frac{\sigma}{r_{ij}} \right)^{12} - \left(\frac{\sigma}{r_{ij}} \right)^6 \right], \quad (1)$$

Table 1. The nanojet system dimensions and atoms used.

Aperture type	Length (nm)	Width (nm)	Push panel atoms	Plate atoms	Total atoms
A (maximum)	3.530 15	2.987 05	624	12 800	21 620
B (large)	2.987 05	2.443 95	624	12 800	21 680
C (middle)	2.443 95	1.900 85	624	12 800	21 728
D (small)	1.900 85	1.357 75	624	12 800	21 764

where $\phi(r_{ij})$ is a pair energy function, r_{cut} (the cut-off distance) is set at 3.5σ , $\sigma = 3.40 \times 10^{-10}$ m and $\varepsilon = 1.67 \times 10^{-21}$ J.

According to the *NTV* model the nanojet housing temperature must remain constant, but the following correction was required in order to attain a constant temperature:

$$v_i^{\text{new}} = v_i \sqrt{\frac{T_D}{T_A}}, \quad (2)$$

where v_i^{new} is the velocity of the particle i after correction. T_D and T_A are the desired temperature and actual temperature of the system, respectively. The time integration of motion is performed by Gear's fifth predictor–corrector method [20] with a time step of 1 fs. In this simulation, the atoms are deposited on a solid plate and the plate can be fixed or moved on a horizontal plane.

3. Results and discussions

The snapshots of the nanojet ejected droplets onto a fixed solid surface using a type B aperture, at a temperature of $T = 200$ K and measured at various sampling times are shown in figures 2(a)–(d). These figures are 3D projections onto a plane. It was seen that the amount of atoms on the plate increased as the time increased. The expanding atomic behaviours were like those of a free jet expanding into a perfect vacuum before reaching the solid plate. As the ejection droplets reached the surface of the solid plate, the spreading and sputtering behaviours of the atoms took place.

Figures 3(a)–(d) depict the effects of the aperture size on the deposited droplets' configuration at the time step of 70 ps. The area covered by the spreading droplets becomes larger as the aperture size is increased. It was found that the layer phenomenon took place as the atoms were spreading on the plate. The layer phenomenon was found to be strongest when using the type C aperture. The layer phenomenon appears when the velocity of deposition on the solid surface is larger than that of wetting on the same surface. The velocities of deposition and wetting were dependent on the aperture size, sampling time and number of atoms in the interior and on the plate surface, etc. Furthermore, the larger nozzle aperture sizes showed that more evaporation of the ejected Ar liquid took place.

Figure 4 illustrates the relationship of the droplets' spreading width and the time steps for the different aperture dimensions. When the atoms were deposited on a solid plate, the spreading width increased as time and the nozzle aperture dimensions increased.

The contact angles of the spreading droplets varied with time for the four different aperture dimensions used as depicted in figure 5. The contact angle is defined as the angle formed at the intersection of the droplets with the solid surface and is a key measurement needed to determine the shape of the fluid on the solid interface. At the start time the contact angle was 180° and then the angle decreased as the time increased. In figure 5 the sampling time shown is from 20 to 80 ps for convenient comparison, when the contact angles for the four cases were

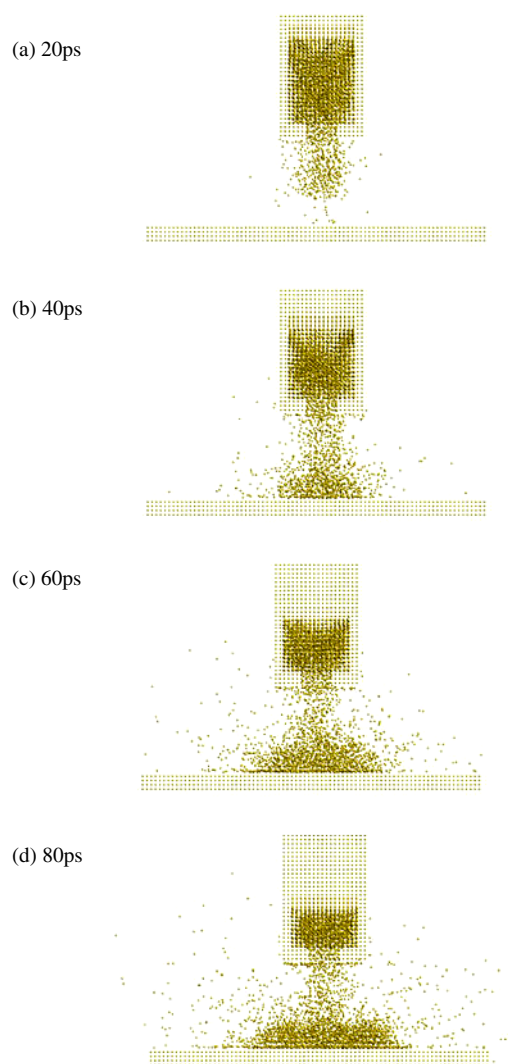


Figure 2. Snapshots of the ejected droplet onto a fixed solid surface using an aperture type B at $T = 200$ K at various sampling times.

near 90° . The contact angle gradually reached a relatively steady state and the variation of the contact angle ranged from about 30° to 60° .

Figure 6 shows the energy variations for the different aperture dimensions. The wave phenomenon of the energy was found and may have resulted from the pressure variation of the interior atoms or the background pressure that was formed by the effused and ejected atoms. The push panel had a velocity of 50 m s^{-1} originating from the back of the system and was not continuously pushing on the atoms. This then caused the atoms to vibrate at a frequency of 93.5 GHz , which then induced a pressure variation within the atoms, causing the wave phenomenon that can be seen in the energy–time curve. After 20 ps higher energies exist in the atoms for the smallest (type D) aperture used.

The thin films deposited onto a moving solid surface are shown in figures 7(a)–(e). The solid surface is moved at a velocity of 200 m s^{-1} . After several tens of picoseconds, the thin

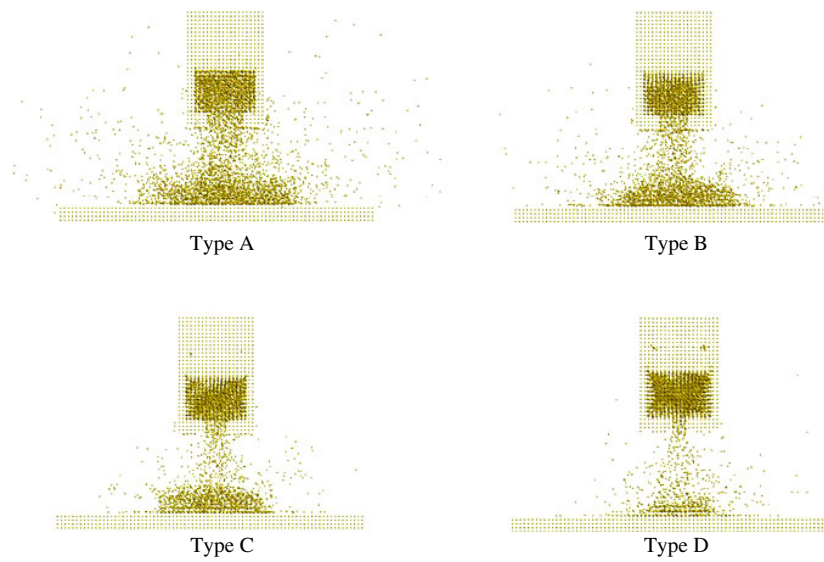


Figure 3. The effect of aperture size on the deposited droplets' configuration at the time step of 70 ps.

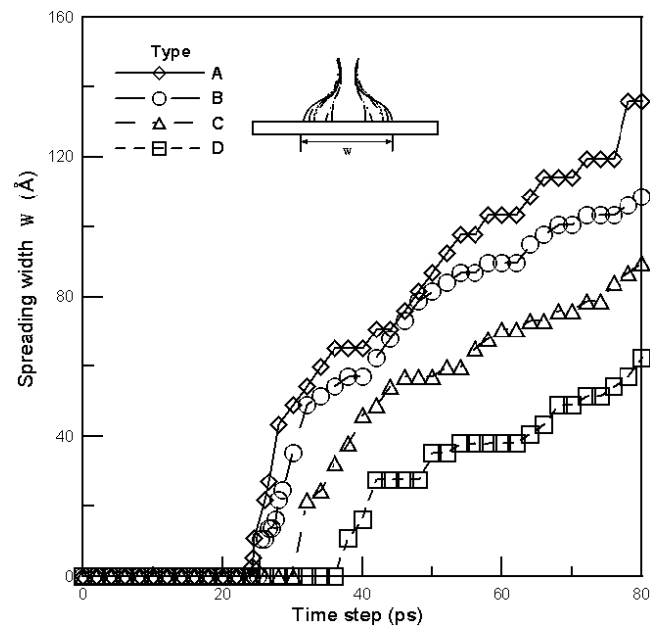


Figure 4. The relationship of the spreading width of the droplets and the time steps for the four different aperture dimensions used.

film on the solid surface gradually begins to form what is known as the layer phenomenon. The thinner film can be obtained when the solid surface is moving at higher velocities. The behaviour of this process may be improved for deposition application using molecular beam epitaxy.

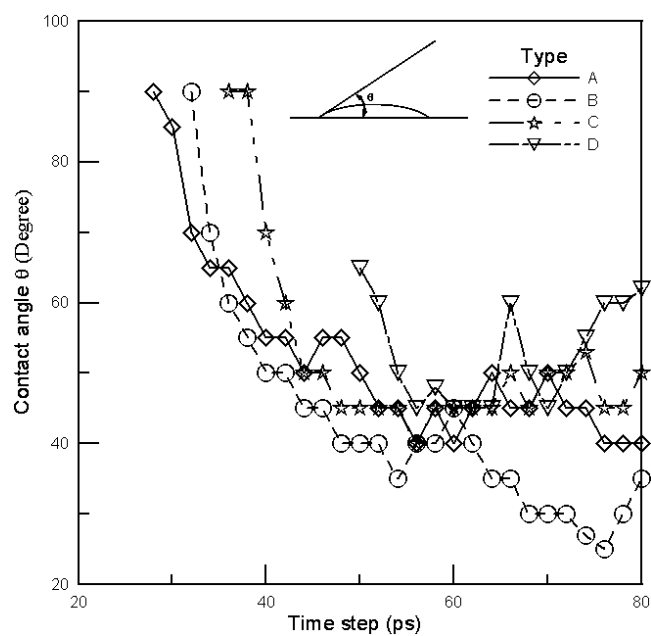


Figure 5. The droplets' contact angle with the surface at different time steps using four different aperture dimensions.

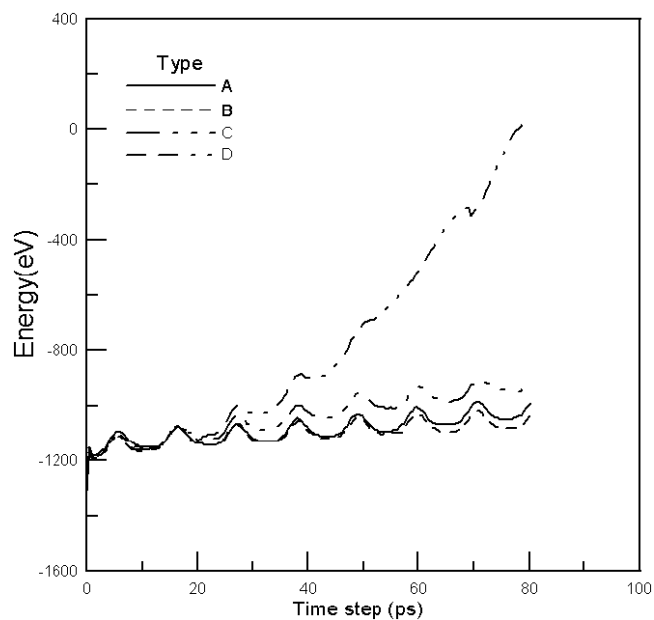


Figure 6. The energy variations at different aperture dimensions.

4. Conclusions

The molecular dynamics method was successfully applied to simulate the spreading of droplets on a solid surface using nanojets. Based on the simulation, the following results were obtained:

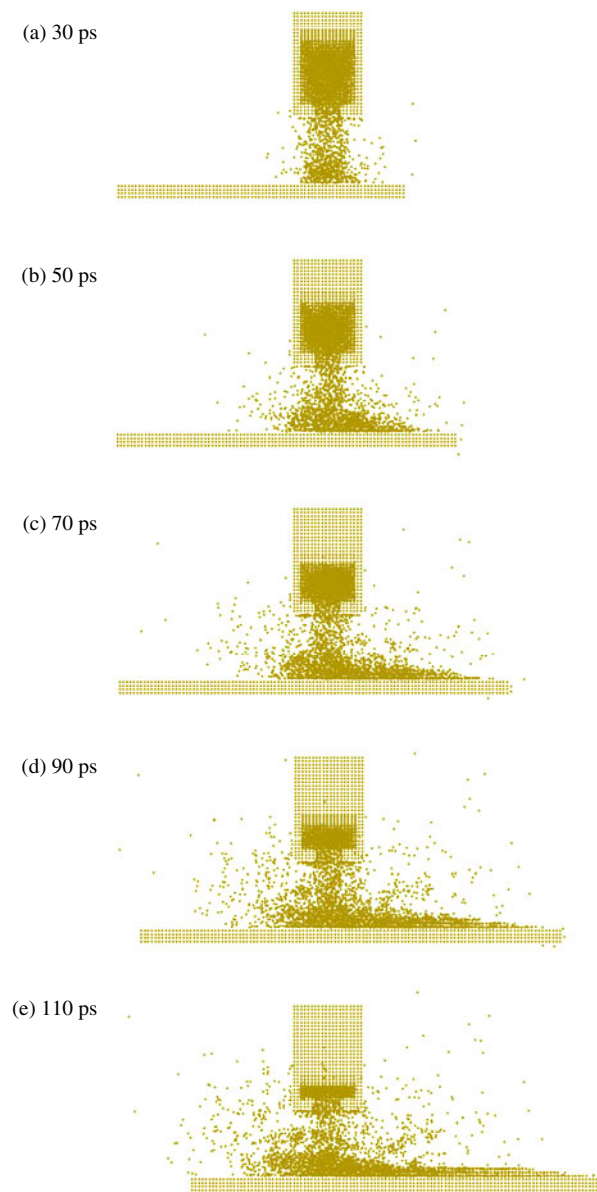


Figure 7. Thin film deposited on a moving solid surface.

- (1) As the aperture dimensions and time increased, the spreading widths increased.
- (2) The energy wave phenomenon occurred and it showed that the energy varied with time.
- (3) When the atoms in the injection process reached a relatively steady state, the variation of the contact angle ranged from about 30° to 60° .
- (4) When the thin films were deposited on a moving plate, the layer phenomenon became apparent.

Acknowledgments

The authors wish to thank the National Science Council of the Republic of China in Taiwan for providing financial support for the present study through project NSC 92-2212-E-168-010.

References

- [1] Yasuoka K, Matsumoto M and Kataoka Y 1994 *J. Chem. Phys.* **101** 7904
- [2] Rytönen A, Valkealahti S and Manninen M 1997 *J. Chem. Phys.* **106** 1888
- [3] Yamaguchi N, Sasajima Y, Terashima K and Yoshida T 1999 *Thin Solid Films* **345** 34
- [4] Fichtmuller M, Corrigan G, Lauro-Taroni L, Simonini R, Spence J, Springmann E and Taroni A 1999 *J. Nucl. Mater.* **330** 266–9
- [5] Korlie M S 2000 *Comput. Math. Appl.* **39** 43
- [6] Fang T H and Weng C I 2000 *Nanotechnology* **11** 148
- [7] Chang W J 2003 *Microelectron. Eng.* **65** 239
- [8] Chang W J and Fang T H 2003 *J. Phys. Chem. Solids* **64** 1279
- [9] Summers D A 1995 *Waterjetting Technology* (London: Spon)
- [10] Eggers J 1997 *Rev. Mod. Phys.* **69** 865
- [11] Hayes D J, Cox W R and Grove M E 1998 *J. Electron. Manuf.* **8** 209
- [12] Moseler M and Landman U 2000 *Science* **289** 1165
- [13] Eggers J 2002 *Phys. Rev. Lett.* **89** 084502
- [14] Joanny J F and de Gennes P G 1986 *J. Physique* **47** 121
- [15] de Gennes P G, Hua X and Levinson P 1990 *J. Fluid Mech.* **212** 55
- [16] Tanner L H 1979 *J. Phys. D: Appl. Phys.* **12** 1473
- [17] Blake T D, Clarke A, De Coninck J, de Ruijter M and Voue M 1999 *Colloids Surf. A* **149** 123
- [18] Edmund B W III and Gary S G 2002 *Scr. Mater.* **47** 393
- [19] Hoover W G 1985 *Phys. Rev. A* **31** 1695
- [20] Haile J M 1992 *Molecular Dynamic Simulation* (New York: Wiley)